IET Nanobiotechnology

Research Article

IET Journals
The Institution of Engineering and Technology

Eco-friendly synthesis of silver and gold nanoparticles with enhanced antimicrobial, antioxidant, and catalytic activities

ISSN 1751-8741
Received on 19th December 2017
Revised 9th March 2018
Accepted on 3rd April 2018
E-First on 1st May 2018
doi: 10.1049/iet-nbt.2017.0311
www.ietdl.org

Remya Vijayan[1], Siby Joseph[2], Beena Mathew[1] ✉

[1]*School of Chemical Sciences, Mahatma Gandhi University, Kottayam 686560, Kerala, India*
[2]*Department of Chemistry, St. George's College, Aruvithura, Kottayam 686122, Kerala, India*
✉ *E-mail: beenamscs@gmail.com*

Abstract: The present work is emphasised on the bio-fabrication of silver and gold nanoparticles in a single step by a microwave-assisted method using the leaf extract of *Synedrella nodiflora* as both reducing and stabilising agent. The synthesised nanoparticles are highly stable and show surface plasmon resonance peak at 413 and 535 nm, respectively, for silver and gold nanoparticles in UV–Vis spectrum. The functional group responsible for the reduction of metal ions were obtained from Fourier transform infrared spectroscopy. The crystalline nature of nanoparticles with face-centred cubic geometry was confirmed by the X-ray diffraction and selected area electron diffraction patterns. The morphology and sizes of the silver and gold nanoparticles were obtained from transmission electron microscopy images. The nanoparticles exhibit effective antimicrobial activities against various pathogenic strains. These antimicrobial properties were analysed by employing agar well diffusion method. The nanoparticles show significant antioxidant properties, and it was determined using 2, 2-diphenyl-1-picrylhydrazyl assay. The nanoparticles also show potent catalytic activity in the degradation of anthropogenic pollutant dyes Congo red and eosin Y by excess $NaBH_4$. Thus, the current study demonstrates the potential use of *S. nodiflora* as a reducing and stabilising agent for the synthesis of silver and gold nanoparticles and their relevance in the field of biomedicine and catalysis.

1 Introduction

Nanotechnology is a branch of interdisciplinary research on particles in the size range 1–100 nm and is engaged with the design of nanoscale structures for advanced applications [1]. The nanoparticles exhibit new peculiar properties contrast to the large particles of bulk material [2, 3] and has potential applications in various industrial, biomedical, and electronic fields [4]. Noble metal nanoparticles like gold, silver, platinum, and palladium gained huge attention because of their extraordinary electronic, chemical, and optical properties [5–7]. Various physical and chemical process like laser radiation [8], sonochemical method [9], co-precipitation [10], inverse microemulsions [11], ultrasound irradiation [12], and chemical reduction [13] have been reported for the synthesis of metal nanoparticles. All these methods require dangerous chemicals, noxious solvents, high temperature and pressure conditions, and so on [14–16]. However, biological methods are very simple, eco-friendly, and do not require toxic reducing and stabilising agents, therefore this method is widely used [17, 18].

Metal nanoparticles have been prepared through various biological approaches using microorganisms [19–21], enzymes [22], and plant materials [23–25]. Among these biological methods, plant-mediated synthesis is very simple and do not require any complicated process as in other methods [26]. The variety of biomolecules like phenols, proteins, flavonoids present in the plant extract can act as reducing and stabilising agent for the nanoparticles formation [27]. These days, a large number of plants are effectively used for the simple, rapid, and cost effective synthesis of silver and gold nanoparticles [28–32].

In contrast with chemical methods, the biological methods are very slow. This drawback is being overcome by using microwave assisted biosynthetic method without perturbing the green reaction condition. The microwave assisted synthesis has many advantages such as small reaction time, lower energy expenditure, and so on [33, 34]. Microwave irradiation gives fast and consistent heating of the reaction medium and this results in the homogeneous nucleation and development conditions for nanoparticles formation [35]. Several reports on the synthesis of silver and gold nanoparticles based on the microwave-aided method have been published in recent years [36–38].

A large number of organic dyes are used in textile, paint, paper, food, leather, plastic, and cosmetics industries. Most of these dyes are very hazardous and can cause severe environmental pollution problems. Also, it causes serious threats to aquatic systems and human health. Since organic dyes have complex aromatic structure and high stability, it cannot be removed by conventional treatment techniques like ultra-filtration, adsorption, reverse osmosis, coagulation, and so on [39]. So the removal of the dyes is one of the challenging task faced by environmentalists. Use of nanocatalyst for the removal of dye pollutant is a simple technique and can be applied in mild conditions, so this method is widely used in recent years [40]. The nanoparticles can act as an effective catalyst due to their small size, high surface to volume ratio, and size-dependent activity [41, 42].

Synedrella nodiflora is a medicinal plant that belongs to the family of Asteraceae or Compositae. It exhibits strong antioxidant potential, antifeedant efficiencies, anti-inflammatory effect, insecticidal, analgesic, and antipyretic activity [43, 44]. Additionally, its leaves are used for the treatment of rheumatism, earache, stomach ache, and so on [45]. The aqueous extract of *S. nodiflora* contains reducing sugars, alkaloids, phenolic compounds, saponins, tannins, and aromatic acids [46].

In this study, we explained an easy and single step method for the rapid synthesis of silver and gold nanoparticles by reducing the corresponding metal salt using the aqueous leaf extract of *S. nodiflora* with the aid of microwave radiation. The leaf extract acts as both reducing and stabilising agent for the formation of nanoparticles. The reports on the synthesis of silver nanoparticles using the leaf extract of *S. nodiflora* by sunlight irradiation [47] and heating [48] methods are already available. However, the novelty of the present work lies in the usage of *S. nodiflora* leaf extract for the synthesis of silver and gold nanoparticles by microwave irradiation and which results in the formation of nanoparticles in <30 s of time. To the best of our knowledge, green synthesis of silver and gold nanoparticles using *S. nodiflora* leaf

extract as reducing and stabilising agent by microwave irradiation has not yet been reported. The main focus of this study is the evaluation of antimicrobial, antioxidant, and catalytic activities of synthesised nanoparticles. The antioxidant activities were measured by using the DPPH assay. The antimicrobial test was conducted on six microbial strains by using the agar well diffusion method. The catalytic activities of silver and gold nanoparticles towards the reduction of aromatic dyes Congo red (CR) and eosin Y (EY) were also reported. The nanoparticles exhibited good catalytic activity and were found to follow pseudo first-order kinetics.

2 Materials and methods

2.1 Chemicals

Silver nitrate ($AgNO_3$), 2, 2-diphenyl-1-picrylhydrazyl (DPPH), ascorbic acid, CR, EY were purchased from Merck Chemicals, India. The hydrogen tetrachloroaurate (III) trihydrate ($HAuCl_4.3H_2O$) and sodium borohydride ($NaBH_4$) were obtained from Sigma Aldrich. All chemicals were used as such without further purifications.

2.2 Preparation of S. nodiflora leaf extract

The fresh leaves of *S. nodiflora* were collected and taxonomically identified. For preparing the aqueous *S. nodiflora* leaf extract for biosynthesis, 25 g of freshly collected and thoroughly washed leaves were incised into small pieces and taken in an round-bottom flask. About 100 ml of double distilled water was added to it and the mixture was boiled for 20 min at 60°C. Then the filtrate was cooled and filtered through Whatman No.1 filter paper. The filtrate was then stored at 4°C in a refrigerator until further use.

2.3 Biosynthesis of silver and gold nanoparticles

Silver and gold nanoparticles were synthesised with the aid of microwave irradiation. For this, 10 ml of *S. nodiflora* leaf extract was mixed with 90 ml of 1 mM $AgNO_3$/$HAuCl_4.3H_2O$ solution in a 250 ml beaker. Then this solution was placed in a domestic microwave oven (Sharp R-219 T) and was subjected to microwave irradiation. Its operating power and frequency were 800 W and 2450 MHz. The formation of nanoparticles was monitored by using UV–Vis spectrophotometer in the range 200–800 nm. The synthesised silver and gold nanoparticles were, respectively, represented as AgNP-*nodiflora* and AuNP-*nodiflora*.

In order to synthesise nanoparticles at room temperature, 10 ml of *S. nodiflora* leaf extract was mixed with 90 ml of 1 mM $AgNO_3$/$HAuCl_4.3H_2O$ solution in a 250 ml beaker and allowed to react in a room temperature. Then the formation of nanoparticles was monitored by using UV–Vis spectrophotometer in the range 200–800 nm.

2.4 Antimicrobial studies

The agar well diffusion method was used to determine the antimicrobial activity of synthesised nanoparticles [49]. For this, two gram positive bacteria (*Bacillus subtilis* and *Streptococcus* sp.), two gram negative bacteria (*Pseudomonas* sp. and *E. coli*), and two fungi (*Aspergillus* sp. and *Penicillium* sp.) were used. Distilled water was used as a control. All these microorganisms were procured originally from Microbial Type Culture Collection, Institute of Microbial Technology, Chandigarh, India. First, the Petri plates containing 20 ml of media (nutrient agar for bacteria and potato dextrose agar for fungi) were seeded with the matured culture of microorganisms using a sterile cotton swab and allowed to get dry for 10 min. Then four adequately spaced wells (holes) of 6 mm diameter were made per plate using a sterile cork borer and 50 µl of samples (control, *S. nodiflora* leaf extract, AgNP-*nodiflora*, and AuNP-*nodiflora*) were added into the well under aseptic condition. The plates were then incubated at room temperature for nearly one week (fungi) and at 37°C for 24–48 h (bacteria). The antimicrobials present in the samples were diffuse out into the medium and interact with the microorganisms. At the end of the incubation period, the zone of inhibition (ZOI) was calculated to the nearest millimetre. Each test was carried out in three replicates for confirmation of the results.

2.5 Antioxidant studies

DPPH is a stable free radical and is broadly used to study the radical scavenging activity of the antioxidant compounds. The radical scavenging activities of the samples were determined by using DPPH assay according to Chang *et al.* [50]. For this study, different concentrations of samples (12.5–200 µg/ml) were prepared in DMSO and 2.96 ml DPPH (0.1 mM) solution was added to it. Then the reaction mixture was incubated in dark condition at room temperature for 20 min. After 20 min, the absorbance of the mixture was read at 517 nm. DPPH was used as a control and ascorbic acid as standard. The percentage of scavenging activity was calculated by using the following equation: $[(\text{Absorbance}_{\text{control}} - \text{Absorbance}_{\text{sample}})/\text{Absorbance}_{\text{control}}] \times 100$. All experiments were repeated in triplicate and means with standard deviation (SD) were calculated.

2.6 Catalytic studies

The catalytic reduction of organic dyes by $NaBH_4$ was studied as follows. First, 2.5 ml of dye solution (0.1 mM EY/0.3 mM CR) was taken in a quartz cuvette of 1 cm path length. Then it is mixed with ice cold solution of 0.5 ml of 0.06M $NaBH_4$ followed by 0.5 ml (0.02 mg/ml) of AgNP-*nodiflora*/AuNP-*nodiflora* and shaken well. The variation in concentration of dye with time was observed using UV–Vis spectrophotometer by following the change in the absorbance at λ_{max} of the dye solutions. Absorption spectra were recorded at 1 min intervals in the range 200–800 nm.

2.7 Statistical analysis

All biological experiments were carried out three times and the data were represented as the mean ± SD. The data were analysed using one-way analysis of variance followed by Tukey's test (post-hoc test). The results with $P < 0.05$ were considered as statistically significant. The data were statistically analysed with the statistical package, Graph Pad prismV5.

2.8 Characterisation

To characterise the synthesised nanoparticles, several techniques were used. For the UV–Vis spectral studies, Shimadzu UV-2450 spectrophotometer in the range 200–800 nm was used. The phytochemicals that are involved in metal reduction and capping were identified by Fourier transform infrared (FTIR) spectroscopy using Perkin Elmer Spectrum Two spectrometer in the range 500–4000 cm^{-1}. In order to determine the crystalline nature, X-ray diffraction (XRD) analysis was carried out on Bruker AXS D8 Advance X-ray Diffractometer with Cu radiation ($\lambda = 1.5406$ A°). Transmission electron microscopy (TEM) was used to determine the particles size and morphology. JEOL JEM-2100 instrument was used for the TEM analysis. Energy dispersive X-ray (EDX) (for determining elemental composition) was also taken on the same instrument.

3 Results and discussions

3.1 Synthesis of silver and gold nanoparticles and UV–Vis spectral analysis

UV–Vis spectrophotometry is an important technique for determining the formation and stability of nanoparticles in aqueous solutions. Here the formation of silver and gold nanoparticles from their respective salt by aqueous leaf extract of *S. nodiflora* was monitored using UV–Vis spectrophotometric analysis. The photographs of *S. nodiflora* plant, *S. nodiflora* leaf extract, silver nanoparticle (AgNP-*nodiflora*), and gold nanoparticle (AuNP-*nodiflora*) are shown in Fig. 1*a*. The noble metal nanoparticles are known to display unique optical properties due to surface plasmon resonance (SPR) [51]. Upon microwave irradiation for the 30 s, the

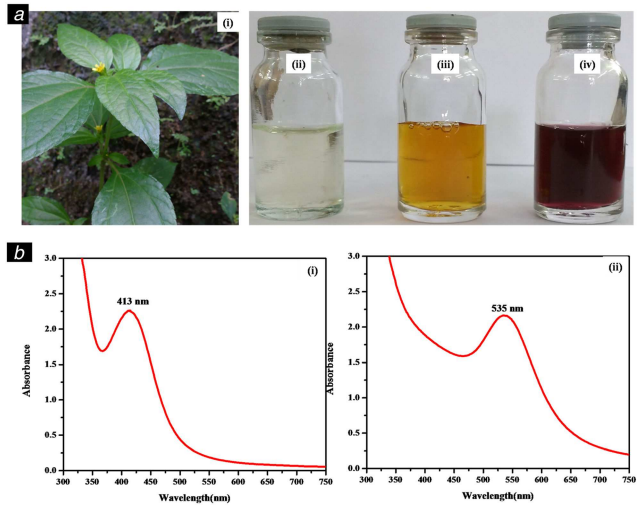

Fig. 1 *Results of visible and UV-vis. spectral analysis*
(a) Photographs of (i) *S. nodiflora* plant, (ii)*S. nodiflora* leaf extract, (iii) AgNP-*nodiflora*, and (iv) AuNP-*nodiflora*, ***(b)*** UV–Vis absorption spectra of (i) AgNP-*nodiflora*, and (ii) AuNP-*nodiflora*

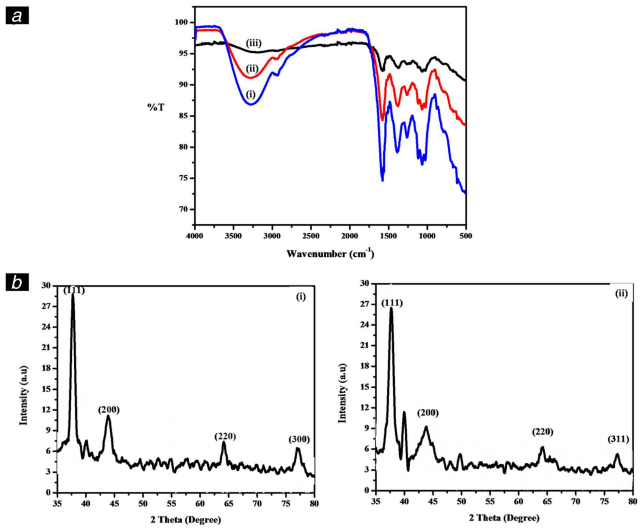

Fig. 2 *Results of FTIR and XRD analysis*
(a) FTIR spectra of (i) *S. nodiflora* leaf extract, (ii) AgNP-*nodiflora*, and (iii) AuNP-*nodiflora*, ***(b)*** XRD pattern of (i) AgNP-*nodiflora*, and (ii) AuNP-*nodiflora*

reaction mixture of silver nitrate and leaf extract getting changed its colour from colourless to pale yellow. This orange colour is attributed to SPR occurring because of the group oscillation of free conduction electrons induced by an interacting electromagnetic field [52, 53]. The SPR band of AgNP-*nodiflora* appeared at 413 nm. The reaction mixture of auric chloride and leaf extract was having slight yellow in colour and upon microwave irradiation of 15 s, its colour is getting changed to blushing red colour and shows SPR at 535 nm in UV–Vis spectrum. The UV–Vis spectra of AgNP-*nodiflora* and AuNP-*nodiflora* are shown in Fig. 1*b*. Here the reduction of metal ions to corresponding nanoparticles occurs via the active molecules present in the leaf extract [54].

In earlier works, the SPR band of silver nanoparticles synthesised by sunlight irradiation was observed at 428.7 nm [47]. The silver nanoparticles synthesised by heating of silver nitrate solution and *S. nodiflora* leaf extract showed SPR peak at 460 nm [48].

In the case of room temperature synthesis, the silver nanoparticles were formed only after 2 h and gold nanoparticles were formed after 1 h.

3.2 FTIR spectral analysis

The FTIR spectra were used to determine the possible functional groups in leaf extract involved in the reduction and stabilisation of synthesised nanoparticles. FTIR spectra of (i) *S. nodiflora* leaf extract, (ii) AgNP-*nodiflora*, and (iii) AuNP-*nodiflora* are shown in Fig. 2*a*. In the case of *S. nodiflora* leaf extract, the major vibrational peaks are found to be located at 3290, 2925, 1680, 1490, 1245, 1033, 1106, and 788 cm^{-1}. The peak at 3290 cm^{-1} could be assigned to –OH vibrations. Peak at 2925 is due to asymmetric stretching vibrations of methylene group. The peak at 1680 cm^{-1} is due to the C = O stretching vibration of the carbonyl and carboxylic groups present in the leaf extract. The band due to symmetrical stretch of carboxylate group is present at 1490. The absorption band at 1245 and 1033 cm^{-1} corresponds to –C–O–C stretching. The peaks at 1106 and 788 cm^{-1} are due to the C–O stretching vibrations of polyols and alcoholic groups. However, after the formation of AgNP-*nodiflora* and AuNP-*nodiflora* the peak become weaker and shifted. The peak at 3290 cm^{-1} shifted to 3269 and 3165 cm^{-1}. The peak at 1680 cm^{-1} is shifted to 1612 and 1590 cm^{-1} also the peak at 1490 is shifted to 1510 and 1515 cm^{-1}. This is suggested that the carbonyl and hydroxyl groups present in the leaf extract are involved in the synthesis and stabilisation of nanoparticles.

3.3 XRD analysis

The crystalline nature of synthesised AgNP-*nodiflora* and AuNP-*nodiflora* was confirmed using XRD analysis. Fig. 2*b*(i) shows the XRD pattern of AgNP-*nodiflora* and Fig. 2*b*(ii) shows the XRD pattern of AuNP-*nodiflora*. There are four reflection peaks observed in the 2θ range 35–80° and this can be indexed to the (111), (200), (220), and (311) reflexions of face centred cubic (fcc) structure of silver (JCPDS file No. 04–0783) and gold (JCPDS file No. 04-0784) nanoparticles. In the case of AgNP-*nodiflora*, the peaks observed at 2θ values 37.82°, 43.92°, 64.16°, and 77.25°, and in AuNP-*nodiflora* peaks observed at 37.92°, 43.94°, 64.30°, and 77.45°. In both cases, the Bragg reflections from (111) plane are more intense than the reflection from other three (200), (220), and (300) planes, which obviously indicates that nanoparticles are mainly oriented along (111) plane [55].

The average crystalline size of the AgNP-*nodiflora* and AuNP-*nodiflora* was calculated using Debye-Scherrer equation [56]

$$D = \frac{K\lambda}{\beta\cos\theta}$$

where 'D' is the particle size, K is the Scherrer constant with a value from 0.9 to 1, 'λ' is the wavelength of X-ray source (0.1541 nm), 'β' is the full width at half maximum, and 'θ' is the diffraction angle that corresponds to lattice plane (111). From the Scherrer equation, the average crystallite size of AgNP-*nodiflora* and AuNP-*nodiflora* was found to be about 15.18 and 19.46 nm, respectively.

3.4 High-resolution TEM (HR-TEM) analysis

The TEM images of the AgNP-*nodiflora* and AuNP-*nodiflora* are, respectively, depicted in Figs. 3 and 4. Here Figs. 3(i) and 4(i), respectively, represents the TEM images of silver and gold nanoparticles. From the TEM images of AgNP-*nodiflora*, it is clear that nanoparticles are highly stabilised and spherical in shape with an average size of 14.16 nm (Fig. 3(iv)). However, in the case of AuNP-*nodiflora*, different morphologies like spherical, triangular, and so on are obtained with average particle size 18.91 nm (Fig. 4(iv)). The clear lattice fringes are revealed in HR-TEM images (Fig. 3(ii) and 4(ii)). The ring like diffraction patterns in selected area electron diffraction (SAED) images (Fig. 3(iii) and 4(iii)) denote that particles are purely crystalline nature (fcc structure). These bright rings originate from the reflection of (111), (200), (220), and (311) planes of fcc silver and gold, which supports the results from the XRD.

The TEM images of nanoparticles synthesised by room temperature method were a little more aggregated when compared to microwave method. The average size of the nanoparticles was obtained as 19.40 nm (AgNP-*nodiflora*) and 22.01 nm (AuNP-

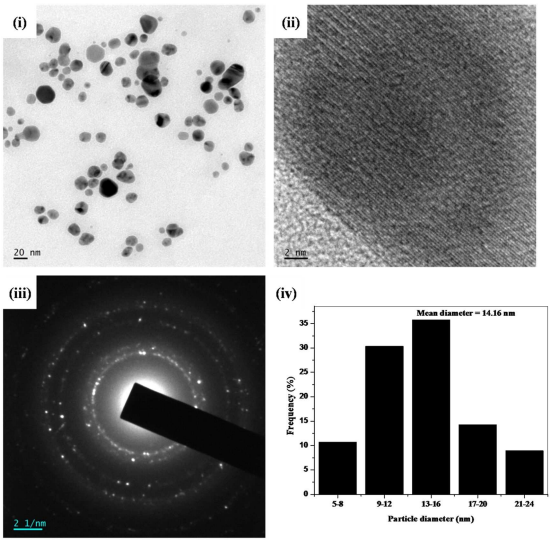

Fig. 3 *(i) TEM image of AgNP-nodiflora, (ii) HR-TEM image, (iii) SAED pattern, and (iv) particle size distribution histogram*

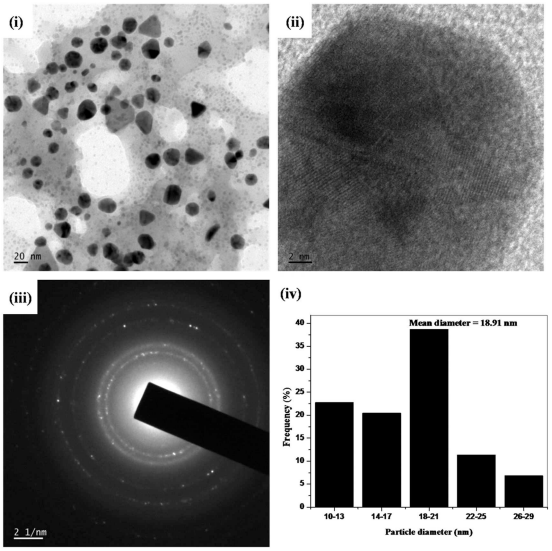

Fig. 4 *(i) TEM image of AuNP-nodiflora, (ii) HR-TEM image, (iii) SAED pattern, and (iv) particle size distribution histogram*

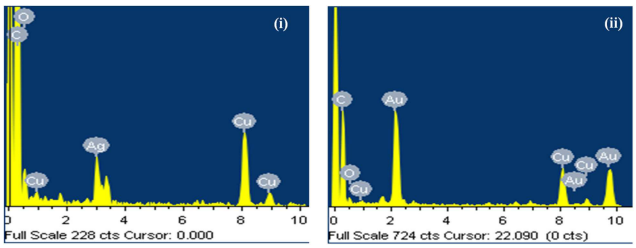

Fig. 5 *EDX spectra of (i) AgNP-nodiflora, and (ii) AuNP-nodiflora*

nodiflora) which is higher than that obtained by microwave method. Thus, the microwave irradiation gives smaller nanoparticles at a faster rate than the room temperature synthesis.

3.5 Energy dispersive X-ray (EDX) analysis

The EDX spectra of synthesised AgNP-*nodiflora* and AuNP-*nodiflora* are shown in Fig. 5. The *X*-axis illustrates the number of X-ray counts and the *Y*-axis illustrates energy in keV. The AgNP-*nodiflora* shows characteristic optical absorption peak approximately at 2.983 keV due to SPR of silver. The AuNP-*nodiflora* showed the signals at around 2.30, 8.10, and 9.40 keV [57]. The signals of carbon and oxygen are also visible in the spectrum, which is originated from the biomolecules of *S.*

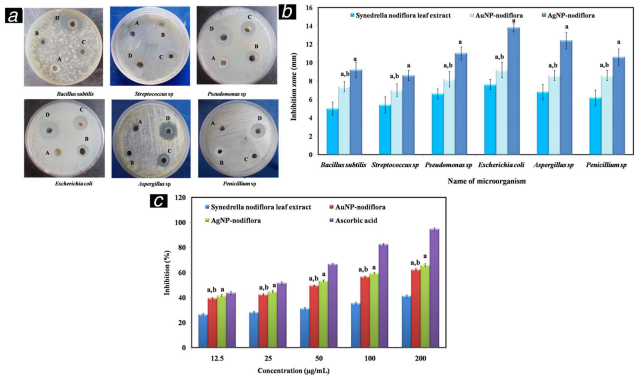

Fig. 6 *Results of antimicrobial and antioxidant studies*

(a) Photographs depicting the antimicrobial activities of *S. nodiflora* leaf extract, AgNP-*nodiflora*, and AuNP-*nodiflora* against different microbial strains (A – control, B – *S. nodiflora* leaf extract, C – AuNP-*nodiflora*, and D – AgNP-*nodiflora*, ***(b)*** Bar diagram depicting the ZOI ($^{a}P < 0.05$, values compared to leaf extract and $^{b}P < 0.05$, values compared to AgNP-*nodiflora*), ***(c)*** Dose-dependent DPPH radical scavenging activity of AgNP-*nodiflora*, AuNP-*nodiflora*, and *S. nodiflora* leaf extract compared to ascorbic acid ($^{a}P < 0.05$, values compared to leaf extract and $^{b}P < 0.05$, values compared to AgNP-*nodiflora*

nodiflora leaf extract. The signals of copper are originated from the copper grid.

3.6 Antimicrobial studies

The inhibitory activities of *S. nodiflora* leaf extract, AgNP-*nodiflora,* and AuNP-*nodiflora* against various pathogens have been studied by using agar well diffusion method. For this two gram positive bacteria (*Bacillus subtilis* and *Streptococcus* sp.), two gram negative bacteria (*Pseudomonas* sp. and *E. coli*), and two fungi (*Aspergillus* sp. and *Penicillium* sp.) were used. Distilled water was used as a control. Fig. 6*a* shows the antimicrobial effect of *S. nodiflora* leaf extract, AgNP-*nodiflora*, and AuNP-*nodiflora* against various microbial pathogens. Bar diagram depicting the ZOI is shown in Fig. 6*b*. From this, it is clear that AgNP-*nodiflora* and AuNP-*nodiflora* have significant antimicrobial activity against all tested microbial strains. The antimicrobial activities of silver and gold nanoparticles have been reported but their precise mechanisms of action are poorly understood. Several mechanisms were proposed for the antimicrobial action of silver and gold nanoparticles. The nanoparticles closely bind to the surface of the microorganisms and make holes in the cell wall. This results in the leakage of cell contents and leads to death [18]. Also, the metal ions could produce free radicals, leading to the rupture of the cell membrane and premature death of the cell [58]. The nanoparticles could also inhibit DNA replication by reacting with the phosphorus or sulphur moieties of DNA [59]. It was reported that the silver nanoparticles synthesised by using *S. nodiflora* leaf extract with the aid of sunlight irradiation and heating methods also showed antimicrobial activities [47, 48].

Also, the bactericidal activities of nanoparticles were higher for gram negative bacteria compared to gram positive bacteria. This is due to the difference in the nature of the cell wall. Gram positive bacteria contain stiff cell wall network with peptidoglycan layer, making it resistant to mechanical rupture, while gram negative bacteria have a cell membrane network that is only one molecule thick [60].

3.7 Antioxidant studies

The antioxidant properties of nanoparticles are very useful in the pharmaceutical industry. Under the normal metabolic process, several reactive oxygen species are continuously produced. If it is not scavenged it causes many medical problems like carcinogenesis, cardiovascular disease, and diabetes mellitus [61, 62]. The reducing agents prevent the generation of reactive oxygen species in the living systems and thus providing an adaptive immunity to several diseases.

The antioxidant potential of *S. nodiflora* leaf extract, AgNP-*nodiflora*, and AuNP-*nodiflora* were measured using the DPPH assay. DPPH (2, 2-diphenyl-1-picrylhydrazyl) is a stable free radical. It will be reduced by accepting electron or hydrogen since the reducing power of a compound is directly proportional to antioxidant activity. The reducing ability of leaf extract and nanoparticles were quantified spectrophotometrically by changing the DPPH colour from purple to yellow using ascorbic acid as a reference. Dose-dependent DPPH radical scavenging activity of AgNP-*nodiflora*, AuNP-*nodiflora*, and *S. nodiflora* leaf extract is presented in Fig. 6*c*. The DPPH activity of the nanoparticles was found to increase in a dose-dependent manner and which is higher than that of leaf extract. At lower concentration of 12.5 µg/ml, *S. nodiflora* leaf extract, AuNP-*nodiflora*, and AgNP-*nodiflora*, respectively, shows 26.38 ± 0.87, 39.32 ± 0.79, and 41.64 ± 0.65 per cent of inhibition. While at higher concentration of 200 µg/ml, they show 41.08 ± 0.89, 62.11 ± 0.9, and 65.91 ± 0.98 per cent of inhibition. IC_{50} values for *S. nodiflora* leaf extract, AuNP-*nodiflora*, and AgNP-*nodiflora*, respectively, were 215, 55.40, and 54.30 µg/ml. The higher free radical inhibition of biosynthesised nanoparticles is due to many reasons like the presence of phytochemicals on the surface, dispersion, and small size [63]. Being more spherical in shape, the antioxidant activities of AgNP-*nodiflora* were higher than that of AuNP-*nodiflora*.

Hence, AgNP-*nodiflora* and AuNP-*nodiflora* shows high biological activities. This is similar to that of previous studies [64, 65].

3.8 Catalytic studies

The catalytic activities of synthesised AgNP-*nodiflora* and AuNP-*nodiflora* were examined using the degradation reactions of dyes CR and EY by $NaBH_4$.

3.8.1 Reduction of CR: CR is a type of azo dye and has a two chromophoric group (azo group), four auxochrome groups (two amino groups and two sodium sulfonate groups). CR is largely used in paper industry and dying of cotton, hemp, silk, and viscose. It is also used as an acid–base indicator, adsorption indicator, and biological stain. It is a carcinogenic and poisonous material. In UV–Vis spectrum of an aqueous solution of CR shows peaks at 490 and 350 nm due to $\pi \rightarrow \pi^*$ and $n \rightarrow \pi^*$ transition of the azo group [66].

Even if sodium borohydride is a strong reducing agent, the aqueous solution of $NaBH_4$ is incapable of reducing CR efficiently due to the huge difference in redox potentials. Thus, the reaction is thermally allowed but kinetically forbidden. The degradation reaction of CR was carried out both in the presence and absence of nanocatalysts. When the reaction is carried out in the absence of nanocatalyst, no change in colour, as well as the intensity, was observed at 490 nm. Successive UV–Vis absorption spectra for the $NaBH_4$ reduction of CR recorded at 1 min intervals without nanocatalysts are shown in Fig. 7(i). From this, it is clear that this dye is not degraded by $NaBH_4$ alone. However, when a few amounts of nanocatalysts were added the degradation reaction was significantly augmented.

Fig. 7(ii and iii) shows the successive UV–Vis absorption spectra of $NaBH_4$ reduction of CR in the presence of nanocatalysts AgNP-*nodiflora* and AuNP-*nodiflora*. From this, it is clear that the intensity of the peak at 490 nm has diminished with time.

The reduction potential of the nanocatalyst is in between those of the dyes (acceptor) and BH_4^- ions (donor) and it makes the electron transfer between them very easy. It can be explained in terms of a Langmuir–Hinshelwood model [67]. First, both the substrates were adsorbed on the catalyst surface. Then, the borohydride ions eject electrons to the surface of the catalyst from which the dye molecules get electrons and hence reduced. Metal nanoparticles have a large surface area to improve the rate of these reduction processes. Also the phytochemicals from the leaf extract attached to the catalytic surfaces also help the adsorption of this substrate on the catalytic surface by electrostatic interaction. The yield of the AgNP-*nodiflora* catalysed reaction was higher than 89% and that of AuNP-*nodiflora* catalysed reaction was higher than 93%.

The kinetics of this reduction reaction was studied spectrophotometrically by examining the intensity of the absorption peak at 490 nm. The amount of reducing agent $NaBH_4$ used in this reaction is much larger than that of CR, and its concentration remains almost constant during the reaction. Therefore the reaction follows pseudo first-order kinetics. The rate equation can be written as $k = 1/t \ln [A_0]/[A]$, where k is pseudo-first order rate constant, $[A_0]$ is the initial concentration of the CR and $[A]$ is the concentration at a time 't'. Thus, the plot of ln $[A]$ versus time 't' gives a straight line with slope k. The plots of ln $[A]$ versus time obtained in the catalytic reduction of CR are shown in the inset of Fig. 7(ii and iii). The details of catalytic reduction of CR by $NaBH_4$ are given in Table 1.

3.8.2 Reduction of EY: EY is a heterocyclic anionic xanthene dye, which contains bromine atoms [tetrabromo fluorescein (or its disodium salt)]. It has many applications in various dyeing, printing, leather, fluorescent pigment, and textile industries, and biomedical research laboratories. The direct release of wastewater containing EY cause many environmental problems and are mutagenic for human beings and animals [68]. The oxidation and reduction reactions of EY were examined from the one-electron reduction and oxidation potentials of its ground state. EY (ES^-_2) decolourises from orange to pale yellow during its reduction to ESH_2 [69].

The reduction of EY by $NaBH_4$ was carried out both in the presence and absence of nanocatalyst to check the role of catalyst in the reaction. It was found that the reduction reaction does not take place in the absence of nanocatalyst. Successive UV–Vis absorption spectra for the $NaBH_4$ reduction of EY recorded at 1 min intervals without nanocatalyst are shown in Fig. 8(i). However, the reduction reaction happened very quickly in the presence of nanocatalyst. This was indicated by the steady decrease in the absorption value of the EY at 515 nm. The nanocatalysts make the kinetically forbidden reduction reaction into allowing one by mediating the electron transfer between the donor borohydride and EY. The reduction potential of the nanocatalyst lies between the dye and borohydride. The UV–Vis spectra for the reduction of CR using AgNP-*nodiflora* and AuNP-*nodiflora* are shown in Fig. 8(ii and iii). The yield of the AgNP-*nodiflora* catalysed reaction was higher than 82% and that of AuNP-*nodiflora* catalysed reaction was higher than 85%.

As the concentration of $NaBH_4$ used in this study largely surpassed that of EY, pseudo-first order kinetics with respect to the concentration of EY was assumed in this case. The plot of ln $[A]$

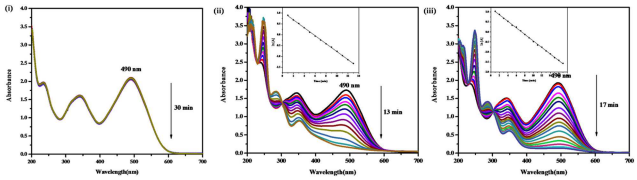

Fig. 7 *(i) Successive UV–Vis absorption spectra for the $NaBH_4$ reduction of CR recorded at 1 min intervals without nanocatalyst, (ii) successive UV–Vis absorption spectra for the $NaBH_4$ reduction of CR recorded at 1 min intervals catalysed by 0.02 mg/ml AgNP-nodiflora, (iii) successive UV–Vis absorption spectra for the $NaBH_4$ reduction of CR recorded at 1 min intervals catalysed by 0.02 mg/ml AuNP-nodiflora at 28°C (plots of ln[A] versus time shown in the inset of corresponding figures)*

Table 1 Details of catalytic reduction of CR by $NaBH_4$

Dye	Nanocatalyst (0.02 mg/ml)	Reaction time, min	Rate constant (k), min^{-1}	Correlation coefficient (R^2)
CR	AgNP-*nodiflora*	13	00.1836	0.9997
	AuNP-*nodiflora*	17	00.1633	0.9995

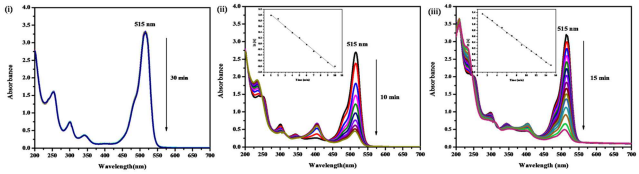

Fig. 8 *(i) Successive UV–Vis absorption spectra for the $NaBH_4$ reduction of EY recorded at 1 min intervals without nanocatalysts, (ii) successive UV–Vis absorption spectra for the $NaBH_4$ reduction of EY recorded at 1 min intervals catalysed by 0.02 mg/ml AgNP-nodiflora, (iii) successive UV–Vis absorption spectra for the $NaBH_4$ reduction of EY recorded at 1 min intervals catalysed by 0.02 mg/ml AuNP-nodiflora at 28°C (plots of ln[A] versus time shown in the inset of corresponding figures)*

Table 2 Details of catalytic reduction of EY by $NaBH_4$

Dye	Nanocatalyst (0.02 mg/ml)	Reaction time, min	Rate constant (k), min^{-1}	Correlation coefficient (R^2)
EY	AgNP-*nodiflora*	10	0.2080	0.9848
	AuNP-*nodiflora*	15	0.1246	0.9813

versus time gives a straight line, and rate constants were directly calculated from the slope of this line. The plots are given in the inset of Fig. 8(ii and iii). The details of catalytic reduction of EY are given in Table 2.

In order to study the reusability of the AgNP-*nodiflora* and AuNP-*nodiflora* catalysts in the dye degradation reactions, the nanocatalysts were recovered from the reaction mixture at the end of the reaction by centrifugation. Then it was dispersed in double distilled water and used for next cycle. The rate of degradation of both CR and EY was found to be more or less the same for up to forth cycles. These results imply the high catalytic activities of synthesised nanoparticles.

4 Conclusions

In summary, we have reported a simple, one pot, and green chemical reduction method for the synthesis of stable silver and gold nanoparticles using the aqueous leaf extract of *S. nodiflora* as reducing and capping agent. This method is a better alternative, which excludes the use of high temperature, pressure, energy, and toxic chemicals in metal nanoparticle synthesis. The antioxidant activities of nanoparticles were investigated using DPPH assay and found that they have remarkable antioxidant properties. The nanoparticles also show excellent antimicrobial properties towards bacterial and fungal strains. Thus, the synthesised silver and gold nanoparticles could have a high potential for use in biological applications. The nanoparticles exhibit outstanding catalytic activities towards the degradation of CR and EY by $NaBH_4$. This degradation ability of nanoparticles helps to remove harmful environmental pollutants.

5 Acknowledgment

The financial assistance of UGC (JRF) to Remya Vijayan is gratefully acknowledged.

6 References

[1] Kumar, B., Smita, K., Cumbal, L., *et al.*: 'Synthesis of silver nanoparticles using Sacha inchi (Plukenetia volubilis L.) leaf extracts', *Saudi J. Biol. Sci.*, 2014, **21**, (6), pp. 605–609

[2] Ramesh, P., Rajendran, A., Meenakshisundaram, M.: 'Green synthesis of zinc oxide nanoparticles using flower extract Cassia auriculata', *J. Nanosci. Nanotechnol.*, 2014, **2**, (1), pp. 41–45

[3] Ahmad, T., Wani, I.A., Lone, I.H., *et al.*: 'Antifungal activity of gold nanoparticles prepared by solvothermal method', *Mater. Res. Bull.*, 2013, **48**, (1), pp. 12–20

[4] Wani, I.A., Khatoon, S., Ganguly, A., *et al.*: 'Silver nanoparticles: large scale solvothermal synthesis and optical properties', *Mater. Res. Bull.*, 2010, **45**, (8), pp. 1033–1038

[5] Kumar, B., Smita, K., Seqqat, R., *et al.*: 'In vitro evaluation of silver nanoparticles cytotoxicity on hepatic cancer (Hep-G2) cell line and their antioxidant activity: green approach for fabrication and application', *J. Photochem. Photobiol. B Biol.*, 2016, **159**, pp. 8–13

[6] Murali Krishna, I., Bhagavanth Reddy, G., Veerabhadram, G., *et al.*: 'Eco-friendly green synthesis of silver nanoparticles using salmalia malabarica: synthesis, characterization, antimicrobial, and catalytic activity studies', *Appl. Nanosci.*, 2016, **6**, pp. 681–689

[7] Wani, I.A., Khatoon, S., Ganguly, A., *et al.*: 'Structural characterization and antimicrobial properties of silver nanoparticles prepared by inverse microemulsion method', *Colloids Surf. B, Biointerfaces*, 2013, **101**, pp. 243–250

[8] Sivakumar, M., Venkatakrishnan, K., Tan, B.: 'Synthesis of glass nanofibers using femtosecond laser radiation under ambient condition', *Nanoscale Res. Lett.*, 2009, **4**, pp. 1263–1266

[9] Wani, I.A., Ahmad, T.: 'Size and shape dependant antifungal activity of gold nanoparticles: a case study of candida', *Colloids Surf. B, Biointerfaces*, 2013, **101**, pp. 162–170

[10] Yang, H., Song, X., Zhang, X., *et al.*: 'Synthesis of vanadium-doped SnO2 nanoparticles by chemical co-precipitation method', *Mater. Lett.*, 2003, **57**, (20), pp. 3124–3127

[11] Ahmad, T., Wani, I.A., Ahmed, J., *et al.*: 'Effect of gold ion concentration on size and properties of gold nanoparticles in TritonX-100 based inverse microemulsions', *Appl. Nanosci.*, 2014, **4**, pp. 491–498

[12] Kundu, S., Panigrahi, S., Praharaj, S., *et al.*: 'Anisotropic growth of gold clusters to gold nanocubes under UV irradiation', *Nanotechnology*, 2007, **18**, pp. 1–7

[13] Song, K.C., Lee, S.M., Park, T.S., *et al.*: 'Preparation of colloidal silver nanoparticles by chemical reduction method', *Korean J. Chem. Eng.*, 2009, **26**, (1), pp. 153–155

[14] Manjamadha, V.P., Muthukumar, K.: 'Ultrasound assisted green synthesis of silver nanoparticles using weed plant', *Bioprocess. Biosyst. Eng.*, 2016, **39**, (3), pp. 401–411

[15] Sunkari, S., Gangapuram, B.R., Dadigala, R., *et al.*: 'Microwave-irradiated green synthesis of gold nanoparticles for catalytic and anti-bacterial activity', *J. Anal. Sci. Technol.*, 2017, **8**, (1), pp. 1–9

[16] Ahmad, T., Wani, I.A., Manzoor, N., *et al.*: 'Biosynthesis, structural characterization and antimicrobial activity of gold and silver nanoparticles', *Colloids Surf. B, Biointerfaces*, 2013, **107**, pp. 227–234

[17] Khan, M.N., Khan, T.A., Khan, Z., *et al.*: 'Green synthesis of biogenic silver nanomaterials using Raphanus sativus extract, effects of stabilizers on the morphology, and their antimicrobial activities', *Bioprocess. Biosyst. Eng.*, 2015, **38**, (12), pp. 2397–2416

[18] Reddy, G.B., Madhusudhan, A., Ramakrishna, D., *et al.*: 'Green chemistry approach for the synthesis of gold nanoparticles with gum kondagogu: characterization, catalytic and antibacterial activity', *J. Nanostructure Chem.*, 2015, **5**, (2), pp. 185–193

[19] Das, V.L., Thomas, R., Varghese, R.T., *et al.*: 'Extracellular synthesis of silver nanoparticles by the Bacillus strain CS 11 isolated from industrialized area', *3 Biotech*, 2014, **4**, (2), pp. 121–126

[20] Kushwaha, A., Singh, V.K., Bhartariya, J., *et al.*: 'Isolation and identification of *E. coli* bacteria for the synthesis of silver nanoparticles: characterization of the particles and study of antibacterial activity', *Eur. J. Exp. Biol.*, 2015, **5**, (1), pp. 65–70

[21] Syed, A., Saraswati, S., Kundu, G.C., *et al.*: 'Biological synthesis of silver nanoparticles using the fungus Humicola sp. and evaluation of their cytotoxicity using normal and cancer cell lines', *Spectrochim. Acta A, Mol. Biomol. Spectrosc.*, 2013, **114**, pp. 144–147

[22] Gholami-Shabania, M., Shams-Ghahfarokhi, M., Gholami-Shabani, Z., *et al.*: 'Enzymatic synthesis of gold nanoparticles using sulfite reductase purified from Escherichia coli: a green eco-friendly approach', *Process Biochem.*, 2015, **50**, (7), pp. 1076–1085

[23] Joseph, S., Mathew, B.: 'Microwave-assisted green synthesis of silver nanoparticles and the study on catalytic activity in the degradation of dyes', *J. Mol. Liq.*, 2015, **204**, pp. 184–191

[24] Patra, J.K., Das, G., Baek, K.H.: 'Phyto-mediated biosynthesis of silver nanoparticles using the rind extract of watermelon (Citrullus lanatus) under photo-catalyzed condition and investigation of its antibacterial, anticandidal and antioxidant efficacy', *J. Photochem. Photobiol. B Biol.*, 2016, **161**, pp. 200–210

[25] Vijayan, R., Joseph, S., Mathew, B.: 'Green synthesis, characterization and applications of noble metal nanoparticles using Myxopyrum serratulum A. W. Hill leaf extract', *Bionanoscience*, 2018, **8**, (1), pp. 105–117

[26] Sathishkumar, P., Vennila, K., Jayakumar, R., *et al.*: 'Phyto-synthesis of silver nanoparticles using Alternanthera tenella leaf extract: an effective inhibitor for the migration of human breast adenocarcinoma (MCF-7) cells', *Bioprocess Biosyst. Eng.*, 2016, **39**, (4), pp. 651–659

[27] Maria, B.S., Devadiga, A., Kodialbail, V.S., *et al.*: 'Synthesis of silver nanoparticles using medicinal Zizyphus xylopyrus bark extract', *Appl. Nanosci.*, 2015, **5**, (6), pp. 755–762

[28] Vijayan, R., Joseph, S., Mathew, B.: 'Indigofera tinctoria leaf extract mediated green synthesis of silver and gold nanoparticles and assessment of their anticancer, antimicrobial, antioxidant and catalytic properties', *Artif. Cells, Nanomed, Biotechnol.*, 2018, **46**, (4), pp. 861–871

[29] Lim, S.H., Ahn, E.-Y., Park, Y.: 'Green synthesis and catalytic activity of gold nanoparticles synthesized by Artemisia capillaris water extract', *Nanoscale Res. Lett.*, 2016, **11**, (1), pp. 1–11

[30] Francis, S., Joseph, S., Koshy, E.P., *et al.*: 'Microwave assisted green synthesis of silver nanoparticles using leaf extract of *elephantopus scaber* and its environmental and biological applications', *Artif. Cells, Nanomed. Biotechnol.*, 2018, **46**, (4), pp. 795–804

[31] Karthik, R., Govindasamy, M., Chen, S.-M., *et al.*: 'Biosynthesis of silver nanoparticles by using Camellia japonica leaf extract for the electrocatalytic

reduction of nitrobenzene and photocatalytic degradation of Eosin-Y', *J. Photochem. Photobiol. B, Biol.*, 2017, **170**, pp. 164–172
[32] Vanaja, M., Gnanajobitha, G., Paulkumar, K.*, et al.*: 'Phytosynthesis of silver nanoparticles by Cissus quadrangularis: influence of physicochemical factors', *J. Nanostruct. Chem.*, 2013, **3**, (1), pp. 1–9
[33] Nadagouda, M.N., Speth, T., Varma, R.S.: 'Microwave-assisted green synthesis of silver nanostructures', *Acc. Chem. Res.*, 2011, **44**, (7), pp. 469–478
[34] Guadie Assefa, A., Adugna Mesfin, A., Legesse Akele, M.*, et al.*: 'Microwave-Assisted green synthesis of gold nanoparticles using Olibanum Gum (Boswellia serrate) and its catalytic reduction of 4-nitrophenol and hexacyanoferrate (III) by sodium borohydride', *J. Clust. Sci.*, 2017, **28**, (3), pp. 917–935
[35] Joseph, S., Mathew, B.: 'Microwave assisted facile green synthesis of silver and gold nanocatalysts using the leaf extract of Aerva lanata', *Spectrochim. Acta A, Mol. Biomol. Spectrosc.*, 2015, **136**, pp. 1371–1379
[36] Joseph, S., Mathew, B.: 'Microwave-assisted facile synthesis of silver nanoparticles in aqueous medium and investigation of their catalytic and antibacterial activities', *J. Mol. Liq.*, 2014, **197**, pp. 346–352
[37] Kahrilas, G.A., Wally, L.M., Fredrick, S.J.*, et al.*: 'Microwave-assisted green synthesis of silver nanoparticles using orange peel extract', *ACS Sustain. Chem. Eng.*, 2014, **2**, (3), pp. 367–376
[38] El-Naggar, M.E., Shaheen, T.I., Fouda, M.M.G.*, et al.*: 'Eco-friendly microwave-assisted green and rapid synthesis of well-stabilized gold and core-shell silver-gold nanoparticles', *Carbohydr. Polym.*, 2016, **136**, pp. 1128–1136
[39] Rajan, A., Vilas, V., Philip, D.: 'Catalytic and antioxidant properties of biogenic silver nanoparticles synthesized using Areca catechu nut', *J. Mol. Liq.*, 2015, **207**, pp. 231–236
[40] Megarajan, S., Ayaz Ahmed, K.B., Rajendra Kumar Reddy, G.*, et al.*: 'Phytoproteins in green leaves as building blocks for photosynthesis of gold nanoparticles: an efficient electrocatalyst towards the oxidation of ascorbic acid and the reduction of hydrogen peroxide', *J. Photochem. Photobiol. B, Biol.*, 2016, **155**, pp. 7–12
[41] Ghosh, S.K., Kundu, S., Mandal, M.*, et al.*: 'Silver and gold nanocluster catalyzed reduction of methylene blue by arsine in a micellar medium', *Langmuir*, 2002, **18**, (23), pp. 8756–8760
[42] Wani, I.A., Ganguly, A., Ahmed, J.*, et al.*: 'Silver nanoparticles: ultrasonic wave assisted synthesis, optical characterization and surface area studies', *Mater. Lett.*, 2011, **65**, (3), pp. 520–522
[43] Wijaya, S., Nee, T.K., Jin, K.T.*, et al.*: 'Antibacterial and antioxidant activities of Synedrella nodiflora (L.) Gaertn. (Asteraceae)', *J. Complement. Integr. Med.*, 2011, **8**, (1), pp. 1–13
[44] Forestieri, A.M., Monforte, M.T., Ragusa, S.*, et al.*: 'Antiinflammatory, analgesic and antipyretic activity in rodents of plant extracts used in African medicine', *Phyther. Res.*, 1996, **10**, pp. 100–106
[45] Bhogaonkar, P.Y., Dagawal, M.J., Ghorpade, D.S.: 'Pharmacognostic studies and antimicrobial activity of Synedrella nodiflora (L.) Gaertn', *Biosci. Discov.*, 2011, **2**, (3), pp. 317–321
[46] Rathi, M.J., Gopalakrishnan, S.: 'Insecticidal activity of aerial parts of Synedrella nodiflora Gaertn (Compositae) on Spodoptera litura (Fab.)', *J. Cent. Eur. Agric.*, 2005, **3**, (2), pp. 223–228
[47] Jash, S.K., Gorai, D., Gangopadhyay, A.: 'Biosynthesis of silver nanoparticles from aqueous leaf extract of Synedrella nodiflora under sunlight irradiation and screening of its antibacterial activity', *Int. J. Pharm. Sci. Nanotechnol.*, 2014, **7**, (3), pp. 2590–2596
[48] Ogunsile, B.O., Labulo, A., Fajemilehin, A.: 'Green synthesis of silver nanoparticles from leaf extracts of paraquetina nigrescens and Synedrella nodiflora and their antimicrobial activity', *Ife J. Sci.*, 2016, **18**, (1), pp. 245–254
[49] Perez, C., Pauli, M., Bazerque, P.: 'An antibiotic assay by the agar well diffusion method', *Acta Biol. Med. Exp.*, 1990, **15**, (1), pp. 113–115
[50] Chang, S.T., Wu, J.H., Wang, S.Y.*, et al.*: 'Antioxidant activity of extracts from Acacia confusa bark and heartwood', *J. Agric. Food Chem.*, 2001, **49**, (7), pp. 3420–3424
[51] Bindhu, M.R., Umadevi, M.: 'Synthesis of monodispersed silver nanoparticles using Hibiscus cannabinus leaf extract and its antimicrobial activity', *Spectrochim. Acta A, Mol. Biomol. Spectrosc.*, 2013, **101**, pp. 184–190
[52] Philip, D., Unni, C., Aromal, S.A.*, et al.*: 'Murraya Koenigii leaf-assisted rapid green synthesis of silver and gold nanoparticles', *Spectrochim. Acta A, Mol. Biomol. Spectrosc.*, 2011, **78**, (2), pp. 899–904
[53] Ajitha, B., Reddy, Y.A.K., Reddy, P.S.*, et al.*: 'Instant biosynthesis of silver nanoparticles using Lawsonia inermis leaf extract: innate catalytic, antimicrobial and antioxidant activities', *J. Mol. Liq.*, 2016, **219**, pp. 474–481
[54] Ahmad, A., Mukherjee, P., Senapati, S.*, et al.*: 'Extracellular biosynthesis of silver nanoparticles using the fungus Fusarium oxysporum', *Colloids Surf. B, Biointerfaces*, 2003, **28**, pp. 313–318
[55] Suman, T.Y., Radhika Rajasree, S.R., Ramkumar, R.*, et al.*: 'The green synthesis of gold nanoparticles using an aqueous root extract of Morinda citrifolia L', *Spectrochim. Acta A, Mol. Biomol. Spectrosc.*, 2014, **118**, pp. 11–16
[56] Ghoreishi, S.M., Behpour, M., Khayatkashani, M.: 'Green synthesis of silver and gold nanoparticles using Rosa damascena and its primary application in electrochemistry', *Phys. E Low-Dimens. Syst. Nanostructures*, 2011, **44**, (1), pp. 97–104
[57] Arunachalam, K.D., Annamalai, S.K., Hari, S.: 'One-step green synthesis and characterization of leaf extract-mediated biocompatible silver and gold nanoparticles from Memecylon umbellatum', *Int. J. Nanomed.*, 2013, **8**, pp. 1307–1315
[58] Kim, J.S., Kuk, E., Yu, K.N.*, et al.*: 'Antimicrobial effects of silver nanoparticles', *Nanomed. Nanotechnol. Biol. Med.*, 2007, **3**, (1), pp. 95–101
[59] Shanmugam, C., Sivasubramanian, G., Parthasarathi, B.*, et al.*: 'Antimicrobial, free radical scavenging activities and catalytic oxidation of benzyl alcohol by nano-silver synthesized from the leaf extract of Aristolochia indica L.: a promenade towards sustainability', *Appl. Nanosci.*, 2015, **6**, (5), pp. 711–723
[60] Elemike, E.E., Onwudiwe, D.C., Fayemi, O.E.*, et al.*: 'Biosynthesis, electrochemical, antimicrobial and antioxidant studies of silver nanoparticles mediated by Talinum triangulare aqueous leaf extract', *J. Clust. Sci.*, 2016, **28**, (1), pp. 309–330
[61] Waris, G., Ahsan, H.: 'Reactive oxygen species: role in the development of cancer and various chronic conditions', *J. Carcinog.*, 2006, **5**, p. 14
[62] Nagajyothi, P.C., Sreekanth, T.V.M., Tettey, C.O.*, et al.*: 'Characterization, antibacterial, antioxidant, and cytotoxic activities of ZnO nanoparticles using Coptidis Rhizoma', *Bioorg. Med. Chem. Lett.*, 2014, **24**, (17), pp. 4298–4303
[63] Sriranjani, R., Srinithya, B., Vellingiri, V.*, et al.*: 'Silver nanoparticle synthesis using Clerodendrum phlomidis leaf extract and preliminary investigation of its antioxidant and anticancer activities', *J. Mol. Liq.*, 2016, **220**, pp. 926–930
[64] Dhayalan, M., Denison, M.I.J., Jegadeeshwari, A.L.*, et al.*: '*In vitro* antioxidant, antimicrobial, cytotoxic potential of gold and silver nanoparticles prepared using *Embelia ribes*', *Nat. Prod. Res.*, 2017, **31**, (4), pp. 465–468
[65] Jiménez Pérez, Z.E., Mathiyalagan, R., Markus, J.*, et al.*: 'Ginseng-berry-mediated gold and silver nanoparticle synthesis and evaluation of their in vitro antioxidant, antimicrobial, and cytotoxicity effects on human dermal fibroblast and murine melanoma skin cell lines', *Int. J. Nanomed.*, 2017, **12**, pp. 709–723
[66] Yokoyama, K., Fisher, A.D., Amori, A.R.*, et al.*: 'Spectroscopic and calorimetric studies of Congo red dye-amyloid peptide complexes', *J. Biophys. Chem.*, 2010, **1**, (3), pp. 153–163
[67] Zhang, H., Li, X., Chen, G.: 'Ionic liquid-facilitated synthesis and catalytic activity of highly dispersed Ag nanoclusters supported on TiO2', *J. Mater. Chem.*, 2009, **19**, (43), pp. 8223–8231
[68] Vignesh, K., Suganthi, A., Rajarajan, M.*, et al.*: 'Visible light assisted photodecolorization of eosin-Y in aqueous solution using hesperidin modified TiO2 nanoparticles', *Appl. Surf. Sci.*, 2012, **258**, (10), pp. 4592–4600
[69] Vidhu, V.K., Philip, D.: 'Catalytic degradation of organic dyes using biosynthesized silver nanoparticles', *Micron*, 2014, **56**, pp. 54–62